Immunoendocrine dysbalance during uncontrolled *T. cruzi* infection is associated with the acquisition of a Th-1-like phenotype by Foxp3^{+} T cells

Florencia B. González [a,1], Silvina R. Villar [a,1], Rodrigo Fernández Bussy [a], Gaëlle H. Martin [b], Louis Pérol [c,d], Romina Manarin [a], Silvana V. Spinelli [a], Caroline Pilon [e], José Laurent Cohen [b,e,f], Oscar A. Bottasso [a], Eliane Piaggio [c,d,g,*,1], Ana R. Pérez [a,*,1]

[a] IDICER-CONICET, Institute of Clinical and Experimental Immunology of Rosario and Immunology Institute, Faculty of Medical Sciences, National University of Rosario, Argentina
[b] INSERM U955, Equipe 21, Créteil, France
[c] INSERM U932, 26 rue d'Ulm, 75005 Paris, France
[d] Institut Curie, Section Recherche, 26 rue d'Ulm, 75005 Paris, France
[e] Université Paris-Est, UMR_S955, UPEC, Créteil, France
[f] AP-HP, Hôpital Henri-Mondor – A. Chenevier, CIC-BT-504, Créteil, France
[g] INSERM Center of Clinical Investigation (CBT507 IGR-Curie), 75005 Paris, France

ARTICLE INFO

ABSTRACT

We previously showed that *Trypanosoma cruzi* infection in C57BL/6 mice results in a lethal infection linked to unbalanced pro- and anti-inflammatory mediators production. Here, we examined the dynamics of CD4^{+}Foxp3^{+} regulatory T (Treg) cells within this inflammatory and highly Th1-polarized environment. Treg cells showed a reduced proliferation rate and their frequency is progressively reduced along infection compared to effector T (Teff) cells. Also, a higher fraction of Treg cells showed a naïve phenotype, meanwhile Teff cells were mostly of the effector memory type. *T. cruzi* infection was associated with the production of pro- and anti-inflammatory cytokines, notably IL-27p28, and with the induction of T-bet and IFN-γ expression in Treg cells. Furthermore, endogenous glucocorticoids released in response to *T. cruzi*-driven immune activation were crucial to sustain the Treg/Teff cell balance. Notably, IL-2 plus dexamethasone combined treatment before infection was associated with increased Treg cell proliferation and expression of GATA-3, IL-4 and IL-10, and increased mice survival time. Overall, our results indicate that therapies aimed at specifically boosting Treg cells, which during *T. cruzi* infection are overwhelmed by the effector immune response, represent new opportunities for the treatment of Chagas disease, which is actually only based on parasite-targeted chemotherapy.

© 2014 Elsevier Inc. All rights reserved.

1. Introduction

Chagas disease, caused by the protozoan parasite *Trypanosoma cruzi* (*T. cruzi*) is one of the most neglected tropical diseases. Millions of people are infected with *T. cruzi* in Latin America. Moreover, it has spread to non-endemic countries as consequence of people migration, representing a new global health problem. Chagas disease presents two clinical phases with a broad range of symptomatology, and can even be lethal in both phases (Coura and Borges-Pereira, 2010; Nunes et al., 2013; Ramirez et al., 2013). Host resistance during *T. cruzi* infection is dependent on a rapid induction of a Th1 inflammatory response, which could be promptly balanced by diverse immuno-endocrine regulatory mechanisms that prevent the pathology mediated by inflammation and facilitate the survival (Roggero et al., 2006; Savino et al., 2007). Among counterregulatory mechanisms, different players have been implicated, such as anti-inflammatory cytokines like IL-10 and TGF-β, Foxp3^{+} regulatory T cells (Treg cells) and endogenous glucocorticoids (Dutra et al., 2014; Roggero et al., 2009; Sathler-Avelar et al., 2009). In the case of Chagas' disease, the role of Treg cells remains controversial (de Araujo et al., 2011; Kotner and Tarleton, 2007; Mariano et al., 2008). Studies in asymptomatic

* Corresponding authors at: IDICER-CONICET, Instituto de Inmunología, Facultad de Ciencias Médicas, Universidad Nacional de Rosario, Santa Fe 3100, 2000 Rosario, Argentina (A.R. Pérez). INSERM U932, 26 rue d'Ulm, 75005 Paris, France (E. Piaggio).
E-mail addresses: eliane.piaggio@curie.fr (E. Piaggio), perez_anarosa@yahoo.com.ar, perez.ana@conicet.gov.ar (A.R. Pérez).
[1] These authors contributed equally to this work.

patients with chronic *T. cruzi* infection show that, compared to symptomatic ones, they have increased Treg cell frequencies (de Araujo et al., 2011; Sathler-Avelar et al., 2009), suggesting a role for Treg cells in the control of immunopathology. In contrast, in mouse models of acute *T. cruzi* infection Treg cells were found to play a limited role in the control of the parasite-associated inflammation and immunopathology (Kotner and Tarleton, 2007; Sales et al., 2008). These findings implied that regulatory mechanisms might be overcome by the effector response, probably by the exposure to stimulatory signals that favors T effector (Teff) cell development.

Among them, IL-2 emerged as a key factor that may influence Treg and Teff cells response (Fehervari et al., 2006). IL-2 signalling is essential for the clonal expansion, functional activity and for eliciting proper Teff cell memory responses (Bachmann et al., 2007). Nevertheless, IL-2 also plays a major role in the peripheral survival and suppressive function of Treg cells (Malek and Bayer, 2004). Noteworthy, autoimmunity and protective immunity develops in the absence of IL-2R signalling, indicating a more essential role of IL-2 for Treg than Teff cells (Malek, 2003). Indeed, Treg cells require only a very low IL-2/IL-2R signalling threshold to support their development and peripheral homeostasis (Yu et al., 2009). This key point is the basis of the development of Treg-targeted therapy by low dose IL-2 administration (Matsuoka et al., 2013).

In addition to IL-2, other cytokines usually associated with Th1, Th2 or Th17 profiles can influence the function and the phenotype of Treg cells. This implies a certain degree of plasticity of Treg cells, since they can express transcription factors and cytokines that are not classical for this population, without losing their suppressor activity (Hall et al., 2013). In particular, Th1-like Treg cells can express IFN-γ and T-bet and seem to be involved in the suppression of Th1 inflammation (Oldenhove et al., 2009). Moreover, more recent studies indicate that the conversion of conventional Treg cells to Treg cells with a Th-effector phenotype might be associated with the downregulation of Foxp3 and the expression of specific cytokines (Zhou et al., 2009). The relevance of these Th1-like Treg cells in the context of infectious diseases still remains controversial. Probably they may exert a regulatory role dampening the exacerbated Th1 response (Oldenhove et al., 2009), or instead promoting a Th1-driven pathology (Zhou et al., 2009).

Endogenous glucocorticoids, mainly corticosterone in mice, are potent inhibitors of the immune response. Of note, we have previously reported comparative studies carried out between resistant BALB/c and susceptible C57BL/6 mice showing that corticosterone release coupled to the immune process is determinant in the course of *T. cruzi* infection. Accordingly, while BALB/c mice exhibited a rapid increase in corticosterone levels following infection and a controlled production of pro-inflammatory cytokines; no major changes were detected in corticosterone concentrations in C57BL/6 mice in the first week of infection, in clear association with an exacerbated production of TNF-α; phenomenon which clearly contributed to their higher mortality. Besides delayed, corticosterone response in C57BL/6 mice is evidently protective and contributes to prolong survival, since the blockade of glucocorticoid receptor and/or adrenalectomy triggering more exacerbated pro-inflammatory cytokine release and also results in a more reduced survival time (Perez et al., 2007; Roggero et al., 2006). This evidence indicated that a subtle balance between endocrine responses and the concomitant immune response is necessary for an efficient defence against *T. cruzi* infection. Since glucocorticoids may also influence the control of an excessive immune response favoring the development of Treg cells (Barrat et al., 2002; Chen et al., 2006; Unger et al., 2009), we suspect that the delayed endocrine response observed in C57BL/6 mice during *T. cruzi* infection might be related with the Treg cells failed expansion.

We previously demonstrated that lethal *T. cruzi* infection in C57BL/6 mice is paradoxically non-linked to parasite burden but with the establishment of a strong pro-inflammatory environment and a delayed release of glucocorticoids (Roggero et al., 2002, 2006; Perez et al., 2007). Here, we extend these studies during *T. cruzi* infection examining the dynamics of Treg and Teff cell interplay in this highly pro-inflammatory environment and examined the role of glucocorticoids on the Treg/Teff balance. We observed that the release of endogenous glucocorticoids occurring in response to *T. cruzi*-driven immune activation was crucial to sustain Treg homeostasis and the Treg/Teff balance. However, the lethal course of disease was associated with the acquisition of a pathogenic Th-1-like phenotype by Foxp3^{+} T cells and by a breakdown of the Treg cell response. Finally, treatment with a combination of IL-2 plus synthetic corticoid (Dexamethasone) induced Treg cell proliferation and the extinction of their Th1-like profile, which were significantly associated to increased survival.

2. Material and methods

2.1. Mice, parasite and infection protocol

C57BL/6 male mice (8–10 weeks of age) and Cbi suckling mice were bred in the animal facilities of School of Medicine of Rosario. All protocols for animal studies were approved by the Institutional Bioethics and Biosecurity Committees (Resolution N° 3913/2008). Ten days before infection and during all procedures mice were housed at the facilities of the Immunology Institute according guidelines provided by the Institutional Committee for Use and Care of Laboratory Animals. C57BL/6 mice were infected with 1000 viable trypomastigotes of the Tulahuén strain of *T. cruzi* in 100 μL of physiological saline by subcutaneous injection. Parasites were maintained by serial passages in Cbi suckling mice.

2.2. Monitoring of acute infection

Bloodstream forms of *T. cruzi* were assessed under standardized conditions, by direct microscopic observation of 5 μL of heparinized tail venous blood at different days post-infection (pi) according to the each experimental schedule. Data were expressed as number of parasites per 50 microscopic fields. Survival time was monitoring daily along infection.

2.3. Pathology evaluation

Hearts and skeletal muscle were removed at different days pi, sliced transversally in three sections, and fixed in buffered formalin. Paraffin-embedded 5 μm sections were stained with hematoxilin and eosin; or with a biotinylated anti-Foxp3 antibody (eBiosciences) followed by streptavidine-HRP secondary antibody and DAB as chromogen. Tissue parasitism and acute myocarditis were evaluated according to previously published protocols (Roggero et al., 2002). The three sections were examined at whole, for all variables, with a 400× magnification. An experienced pathologist blinded to the study groups interpreted data.

2.4. Cytokine and corticosterone assays

Serum cytokines were measured by specific two-site enzyme-linked immunosorbent assay (ELISA) according to the manufactureŕs specifications. ELISA kits for IFN-γ and IL-10, (detection limits 15.6 pg/ml), were purchased from Pharmingen (San Diego, CA, USA). All samples were assayed in duplicate. For corticosterone determinations, mice were housed individually during 1 week before sampling and kept single-caged throughout

the experiments, as previously published (Roggero et al., 2006). Plasma samples were obtained from the tip of the tail between 8 and 10 a.m. Plasma corticosterone levels were assessed by ELISA, according to manufacturer's specifications (IBL, Germany). Detection limit was 0.20 µg/dL.

2.5. Phenotypic analysis by flow cytometry

Mice were first bled out by cardiac puncture and afterwards spleen and draining subcutaneous lymph nodes (dLN) were surgically obtained from each mouse and dissociated in PBS-FBS 3% (Geiner Bio One) using a glass potter. Cellularity of each organ was determined by counting in Neubauer's chamber under 400× magnifications after staining with trypan blue. In same experiments heparinized blood was obtained from the retro-orbital sinus at different days pi to monitoring T cell response. Cells suspensions of each organ (1.10^6 cells in PBS/SFB 3%) or 50 µL of blood were first incubated with anti-FcγIII/II receptor antibody and followed stained with fluorochrome-conjugated antibodies against CD4, CD8, CD25, GITR, CD62L and CD44. Monoclonal antibodies were conjugated with fluorescein isothiocyanate (FITC), phycoerythrin (PE), PE-Cy7, Chlorophyll peridin protein (PerCP), PerCP-Cy5, allophycocyanin (APC), APC-Cy7 and Alexa Fluor 700 (purchased from BD Pharmingen). In a second step, the intracellular labeling against Foxp3 was performed using a staining kit according to the manufacturer's protocol (eBioscience). For nuclear transcription factors (T-bet, GATA-3, ROR-γt) staining monoclonal antibodies conjugated with PE or FITC were used (eBiosciences). Cell proliferation was evaluated staining nuclear Ki-67 using anti-Ki-67 kit (BD Pharmingen) and cell death was stimated by Annexin V Apoptosis Detection Kit I (BD Pharmingen). Cell acquisition was performed on a FACS ARIA II using FACSDiVa software (BD Biosciences). Living cells were gated on the basis of forward- and side cell-scatter. Background staining values obtained with fluorochrome conjugate isotype were subtracted. For each sample, 100,000 events were collected. Data were analyzed using DiVa or FlowJo Version 9.4.4 (TreeStar) softwares.

2.6. Adrenalectomy

Mice were anesthetized with 100 mg/kg ketamine and 2 mg/kg xylazine and afterwards bilateral adrenalectomy was performed via a dorsal approach. Two small incisions were made on each side of the back just below the rib cage and the adrenal glands were removed with curved forceps. Sham mice were operated in a similar manner, but without removing the adrenals. Following the operation, adrenalectomized mice were given 0.9% (wt/vol) sodium chloride in drinking water. The animals were infected 1 week after the surgery. Spleen and subcutaneous dLN were obtained from all mice after 14 days pi.

2.7. Intracellular cytokine staining

Splenocytes were suspended in RPMI 1640 (Sigma Aldrich) supplemented with 10% FBS (Geiner Bio One), 0.2% gentamycin (10 mg/mL, Gibco, NY, USA), 2% penicillin/streptomycin (100 µg/mL and 100 U/mL, respectively, Gibco, NY, USA) and 50 mM of β-mercaptoethanol for *in vitro* stimulation. For basal cytokine detection, single cell suspensions were cultured in triplicate at 1.10^6 cell/mL in a 48-well plate and stimulated with 1 µg/mL of 12-myristate 13-acetate (PMA, Sigma Aldrich), 0.5 µg/mL of ionomycin (Sigma Aldrich) and brefeldin A (GolgiPlug, BD Biosciences) at 37 °C and 5% CO_2. After 4 h, samples were washed twice with PBS and incubated with anti-FcγIII/II receptor antibody for

30 min and afterwards suspend during 1 h in fixation/permeabilization solution (eBiosciences) according to the manufacturer's instructions and followed stained with PE or FITC-conjugated anti-IL-10 (R&D Systems), anti-IL-17A (BioLegend), anti-IL-4 (BioLegend) and anti-IFN-γ Ab (eBiosciences) in permeabilization buffer. Cell acquisition was performed on FACS ARIA II flow cytometer (Becton Dickinson, San Jose, CA, USA) operating FACSDiVa software (BD Biosciences). For each sample, at least 200,000 events were collected. Living cells were gated on the basis of forward- and side cell-scatter. Background staining values obtained with fluorochrome conjugate isotype were subtracted. Data were analyzed using DiVa or FlowJo Version 9.4.4 (TreeStar) softwares.

2.8. Treatment with IL-2, Dex or combined administration

With the aim of specifically stimulate Treg cells expansion during the course of infection, infected animals were treated with intraperitoneal (ip) injections of low doses (50,000 UI/day) of recombinant human IL-2 (rhIL-2, Proleukin, Novartis) in 100 µL of physiological saline during 5 or 10 consecutive days after *T. cruzi* inoculation. On the other hand and to specifically stimulate Treg cells expansion previously to infection, three different schedules were assessed. Each treatment was done during 7 days. In the first one, mice were treated with daily ip intraperitoneal injections of 50,000 UI of rhIL-2 in 100 µL of physiological saline. In the second one, mice were treated with daily ip injections of 14 µg of Dexamethasone (Dex; Surar Pharma) in 100 µL of physiological saline. In the third one, mice were treated with daily ip injections of both IL-2 plus Dex. Mice injected with PBS were used as non-treated controls. Blood from the retro-orbital sinus was obtained at days 0 and 7 and 14 after treatment whereas spleen and dLNs were obtained from all mice after 14 days of treatment. In same experiments, after 7 days of treatment completion, mice were infected as detailed before, and blood and lymph organs were obtained at different time-points pi.

2.9. PC61 treatment

Mice were treated ip with 250 µg of anti-CD25 PC61 (eBiosciences) in 50 µL of physiological saline 2 days before parasite infection. Mice injected with PBS acts as controls. Flow cytometry determination of CD25 was performed using the clone 7D4 (eBioscencies).

2.10. Isolation and adoptive transfer of CD4⁺CD25⁺ T cells

CD4⁺CD25⁺ and CD4⁺CD25⁻ T cells were isolated from spleen of uninfected C57BL/6 mice by using Regulatory T cell Isolation kit (Miltenyi) according to manufacturer's instructions. The purity of CD4⁺CD25⁺cells was 95% as assessed by flow cytometry. Intracellular staining indicated that isolated CD4⁺CD25⁺ were 90% Foxp3⁺. Mice received one million of CD4⁺CD25⁺ T cells in PBS by intravenous injection and infected 24 h later with *T. cruzi*.

2.11. RNA isolation, cDNA synthesis and qPCR

Spleens were obtained at different days pi. Total RNA was isolated from cells using TRIzol (Invitrogen) according to the manufacture's recommendations. mRNA levels were determined by RT-qPCR. cDNA was synthesized from 1 µg of total RNA using Superscript III reverse transcriptase (Invitrogen) and specific primers for murine IL-2, IL-6, IL-12p40, IL-23p19, IL-27p28, IL-10 and TGF-β (Invitrogen). PCR reactions were performed in a StepOne™/Plus Real-Time PCR System (Life Technologies) using

SYBRGreen I (Roche) to monitor dsDNA synthesis. Data was normalized using GAPDH cDNA quantification. Primers sequences were:

IL-2 F 5′-CCTGAGCAGGATGGAGAATTACA-3′
IL-2 R 5′-TCCAGAACATGCCGCAGAG-3′
IL-6 F 5′-GAGGATACCACTCCCAACAGACC-3′
IL-6 R 5′-AAGTGCATCATCGTTGTTCATACA-3′
IL-12 p40 F 5′-GGAAGCACGGCAGCAGAATA-3′
IL-12 p40 R 5′-AACTTGAGGGAGAAGTAGGAATGG-3′
IL-23 p19 F 5′-TGCTGGATTGCAGAGCAGTAA-3′
IL-23 p19 R 5′-GCATGCAGAGATTCCGAGAGA-3′
IL-27 p28 F 5′-GGCCATGAGGCTGGATCT-3′
IL-27 p28 R 5′-AACATTTGAATCCTGCAGCCA-3′
IL-10 F 5′-GGTTGCCAAGCCTTATCGGA-3′
IL-10 R 5′-ACCTGCTCCACTGCCTTGCT-3′
TGF-β F 5′-TGACGTCACTGGAGTTGTACGG-3′
TGF-β R 5′-GGTTCATGTCATGGATGGTGC-3′
GADPH F 5′-AGCAATGCATCCTGCACCACCA-3′
GADPH R 5′-ATGCCAGTGAGCTTCCCGTTCA-3′

2.12. Statistical analysis

Results are expressed as mean ± SEM or as median/range according to the variable distribution. Data were analyzed using nonparametric tests (Kruskall–Wallis test for k samples followed by Mann–Whitney U-test for comparisons between two samples). Kaplan Meier and Long Rank test were used to evaluated survival curves. The GraphPad Instat 4.0 software (GraphPad, California, USA) was applied for statistical analyses, and differences were considered significant was when p value was < 0.05.

3. Results

3.1. Acute T. cruzi infection induces a severe depletion of Treg cells and unbalances the Treg/Teff ratio

To evaluate the dynamics of Treg (CD4⁺Foxp3⁺) and Teff (CD4⁺Foxp3⁻) cell responses, C57BL/6 mice were infected subcutaneously with 1000 trypomastigotes of *T. cruzi*. In this model, parasites can be detected in blood after ~7 days pi in some animals, reaching to a 100% of detection after 14 days pi, with their numbers progressively increasing until the death of the animals (Fig. 1a). At day 21 pi, ~25% of mice survive and around 1 week later, mortality reaches 100% (Fig. 1b). We observed that the severity of *T. cruzi* infection was first linked to a rapid increase in serum IFN-γ levels and followed by a delayed systemic production of IL-10 (Fig. 1c). Histological studies carried out in the heart and muscle of infected mice revealed strong infiltrates of mononuclear
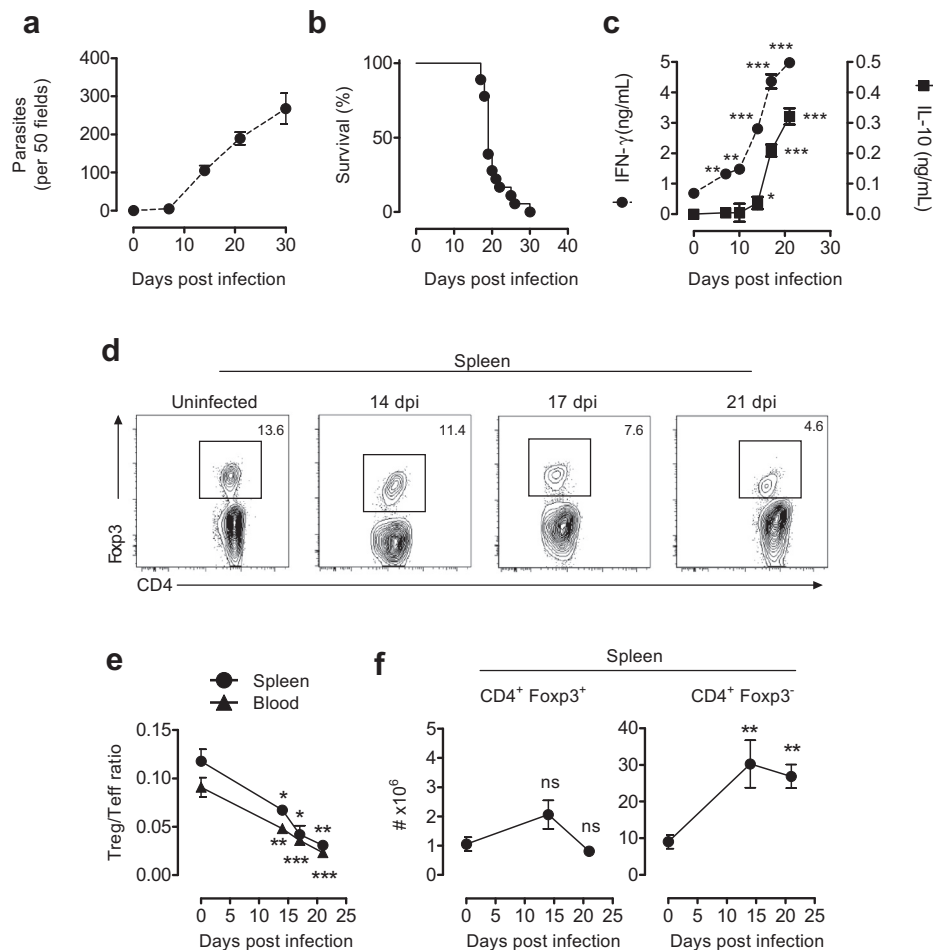

Fig. 1. *T. cruzi*-acute infection induces a systemic pro-inflammatory *milieu* and a diminution in the proportion of Treg cells. (a) Blood parasite burden in C57BL/6 male mice infected subcutaneously with 1000 *T. cruzi* of Tulahuen strain; (b) representative survival curve of infected mice (n = 19); (c) systemic levels of IFN-γ and IL-10 evaluated by ELISA during the course of disease; (d) dot plots illustrating the decrease of CD4⁺Foxp3⁺ Treg cell proportions in the spleen during the course of disease; (e) diminution of blood and splenic Treg (CD4⁺Foxp3⁺)/Teff (CD4⁺Foxp3⁻) cell ratio along infection. (f) absolute number of Treg (CD4⁺Foxp3⁺) and Teff (CD4⁺Foxp3⁻) cells in the spleen after 0, 14 and 21 days pi. For figures c, d, e and f the number of mice examined at each day was 4–8. Results shown are representative of as least three independent experimental rounds. *p < 0.05; **p < 0.01 and ***p < 0.005 vs. day 0.
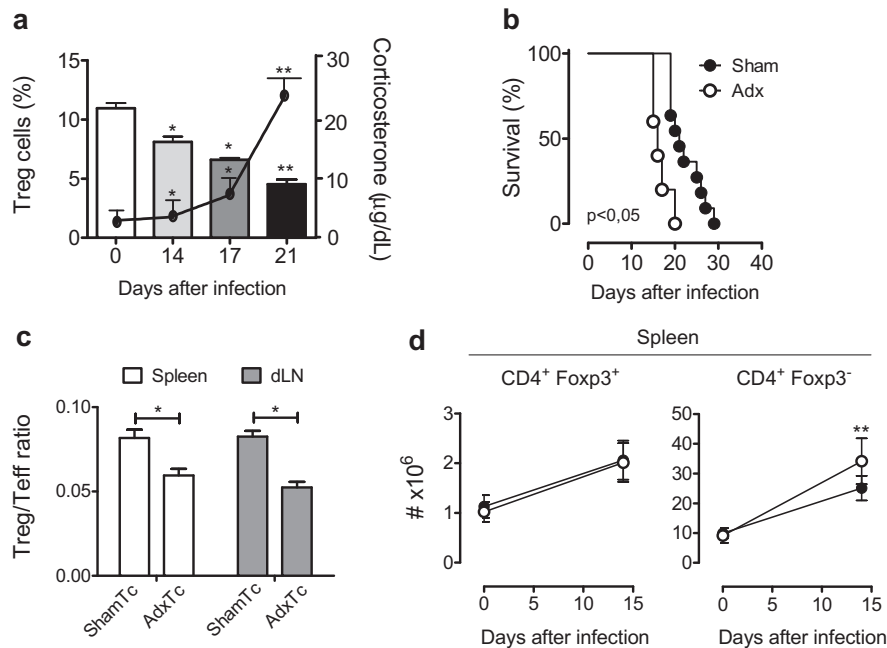
Fig. 2. Corticosterone sustains the Treg/Teff cell ratio during acute *T. cruzi* infection. (a) Spleen Treg (CD4$^+$Foxp3$^+$) cell proportions and their association with corticosterone levels during *T. cruzi* infection ($n = 5$–6/day); $^*p < 0.05$ and $^{**}p < 0.01$ vs. day 0; (b) survival curve of infected C57BL/6 adrenalectomized (Adx) and Sham operated mice. Animals were operated 1 week after infection (Adx, $n = 5$; Sham, $n = 11$); (c) diminution of Treg (CD4$^+$Foxp3$^+$)/Teff (CD4$^+$Foxp3$^-$) cell ratio in the spleen and dLN in Adx and Sham animals after 14 days pi ($n = 3$–4/group); (d) absolute number of Treg and Teff cells. $^*p < 0.05$ between groups. Results shown are representative of at least two independent experimental rounds.

cells, but a scarce occurrence of Foxp3$^+$ cells (*data nor shown*). To evaluate whether the Treg and Teff cell responses were correlated with disease susceptibility and tissue damage, we first analyzed the frequency of both populations in spleen, dLN and blood along infection. Splenic Treg cell proportions gradually decreased along infection, reaching a 3-fold diminution after 21 days pi compared to basal levels (Fig. 1d). Similar results were observed in dLN and blood (*data not shown*). Noteworthy, a marked diminution in the Treg/Teff ratio was observed during the course of disease in spleen and blood (Fig. 1e). In the spleen, the decline of Treg/Teff ratio could be explained by the fact that *T. cruzi* infection results in an increase of Teff but not Treg cell absolute numbers, which remain quite constant along the infection (Fig. 1f). Thus, the striking diminution of the Treg/Teff ratio observed from day 14 pi associated with the scarce number of Treg cells in inflamed peripheral tissues suggests that after 2 weeks of infection Teff cells are unleashed from Treg cell control, likely governing the flared systemic inflammation that ultimately leads to mice death.

3.2. Endogenous glucocorticoids sustain the Treg/Teff cell ratio during acute T. cruzi infection

Of note, previous results from our group showed that glucocorticoid release accompanying *T. cruzi*-driven activation is indispensable to protect the host by impeding an excessive production of pro-inflammatory cytokines (Roggero et al., 2002; Perez et al., 2007). Since, at the same time, glucocorticoids may favor the development of Treg cells (Barrat et al., 2002; Chen et al., 2006; Unger et al., 2009), we evaluated in parallel both parameters along infection. As seen in Fig. 2a, corticosterone secretion remained within physiological levels until day 14 pi, being followed by a substantial increase at days 17 and 21 pi; whereas the proportion of Treg cells continued to decrease. These data suggest that the delayed increase of the GC response observed during the first 2 weeks of infection may be related to the poor Treg cell expansion.

Thus, to understand the role of endogenous corticosterone on Treg cell homeostasis during *T. cruzi* infection, C57BL/6 mice were subjected to bilateral adrenalectomy to deplete mice almost totally from the hormone, or sham surgery, 1 week before infection. Fig. 2b shows that in infected animals, adrenalectomy not only shortened mice survival (Fig. 2b) but also resulted in a diminished Treg/Teff ratio at day 14 pi in both spleen and dLNs compared to sham operated mice (Fig. 2c). The diminution of the Treg/Teff ratio was driven by a diminution in Treg cell frequency (i.e: spleen-14 days pi; infected sham mice = Tregs (%) 7.6 ± 0.3; infected Adx mice = Tregs (%) 4.9 ± 0.2; $p < 0.05$). Interestingly, in infected animals, Adx resulted in increased Teff cell numbers without changes in Treg cell numbers (Fig. 2d). These results indicate that during the two first weeks of *T. cruzi* infection, the relatively low levels of endogenous corticosterone secretion contribute to sustain the Treg/Teff balance.

3.3. Severe T. cruzi infection impairs Treg cell proliferation

The failure of Treg cells to keep up with Teff cell expansion during *T. cruzi* infection, as shown by their declined frequencies, may be related to a diminished proliferation and/or to increased cell death. To test these possibilities, we first compared the proliferation level of splenic Treg and Teff cells during infection. As shown in Fig. 3, after 14 and 19 days pi, the proportion of proliferating Ki-67$^+$ Teff cells and also the proliferative index of Teff cells after 19 days pi were significantly increased during infection, compared to the small rise for Treg cells ($n = 6$/day; Fig. 3a and c-upper panel). In contrast, both populations expressed high levels of the apoptotic marker annexin V and displayed a similar death index after 19 days pi ($n = 6$/day; Fig. 3b and c-bottom panel). These results indicate that compared to Teff cells, Treg cells proliferated to a lower extent during *T. cruzi* infection. To further study the capacity of Treg cells to expand during *T. cruzi* infection we used the PC61 antibody to deplete CD25$^+$ T cells before *T. cruzi*
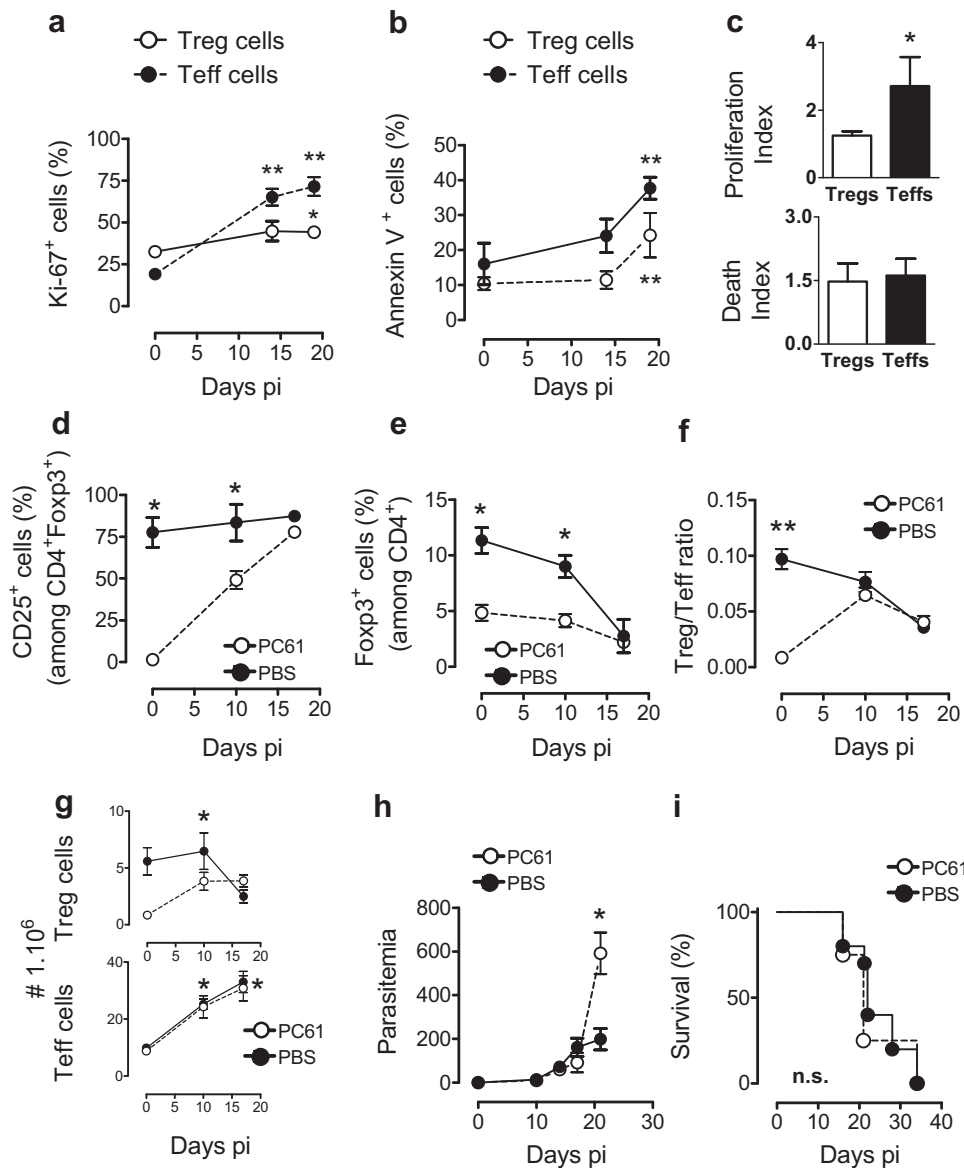
Fig. 3. Severe *T. cruzi* infection impairs Treg cell proliferation. Animals were infected and after different days pi, the spleen were collected and splenocytes were stained for CD4, Foxp3, Ki-67 and annexin V: (a) comparative analysis of Ki-67 proportions between Treg (CD4$^+$Foxp3$^+$) cells and Teff (CD4$^+$Foxp3$^-$) cells after 0, 14 and 19 days pi; (b) comparative analysis of annexin V proportions between Treg (CD4$^+$Foxp3$^+$) cells and Teff (CD4$^+$Foxp3$^-$) cells after 0, 14 and 19 days pi; (c) proliferation index (upper) and death index (bottom). Proliferation and death indexes were calculated as follows: the percentage of Ki-67 positive cells or Annexin V positive cells recorded in each infected mouse divided by the mean percentage recorded in control mice. Index graphs show these data as mean ± SEM. Results shown in figures a, b and c are representative of as least three independent experimental rounds (*n* = 4–5/group/day). Differences between Treg vs. Teff cells at the same day: *$p < 0.05$ and **$p < 0.01$. In another set of experiments, animals were treated with PC61 or PBS on day before infection (*n* = 6–8/group): (d) CD25$^+$ proportions among CD4$^+$ cells one days after PC61 or PBS inoculation (day 0 pi) and 10 and 17 days pi; (e) Foxp3$^+$ expression level in PC61 or PBS treated animals at day 0, 10 and 17 days pi; (f) Treg (CD4$^+$Foxp3$^+$)/Teff (CD4$^+$Foxp3$^-$) cell ratio and, (g) Treg and Teff absolute number determined along the infection in PC61 or PBS treated animals; (h) blood parasite burden in mice treated with PC61 or PBS one day before to infection; (i) survival curve of infected mice (*n* = 6). Results shown are representative of two independent experimental rounds. Differences between PC61 and PBS treated mice at the same day: *$p < 0.05$ and **$p < 0.01$.

inoculation. This schedule of PC61 administration minimizes the depletion of Teff cells, which rapidly express CD25 upon infection. As expected, PC61 treatment before infection totally depleted CD25$^+$ T cells from blood and lymphoid organs by the time of *T. cruzi* inoculation (Fig. 3d). However, it only depleted ∼60–70% of Foxp3$^+$ expressing T cells. Upon infection, the proportion of remaining and/or induced Treg cells rapidly decreased, reaching similar levels to untreated infected mice by day 17 pi (Fig. 3e). In addition, the Treg/Teff cell ratio attained almost similar levels by day 10 pi in PBS and PC61 infected groups (Fig. 3f). Of note, PC61 treatment enhanced the parasitemia only at the end of acute phase (Fig. 3g) but without worsening the disease outcome (Fig. 3h). Together, these findings indicate that CD25$^+$ cell depletion does

not change the course of *T. cruzi* infection. CD25$^+$ cells maintain their capacity to expand and activate during the acute infection, but are mainly represented by Teff cells. Thus, early since *T. cruzi* infection, although T cells expand, the gradual decrease of the Treg/Teff ratio can be attributed to a selective impairment of Treg cell proliferation compared to Teff cells.

3.4. Upon T. cruzi infection a different distribution of naïve and effector phenotypes is observed between Treg and Teff cells

Teff and Treg cells with an effector or memory-like phenotype arise upon specific antigen recognition and acquire different patterns of recirculation (Dutt et al., 2007; Sallusto et al., 1999;
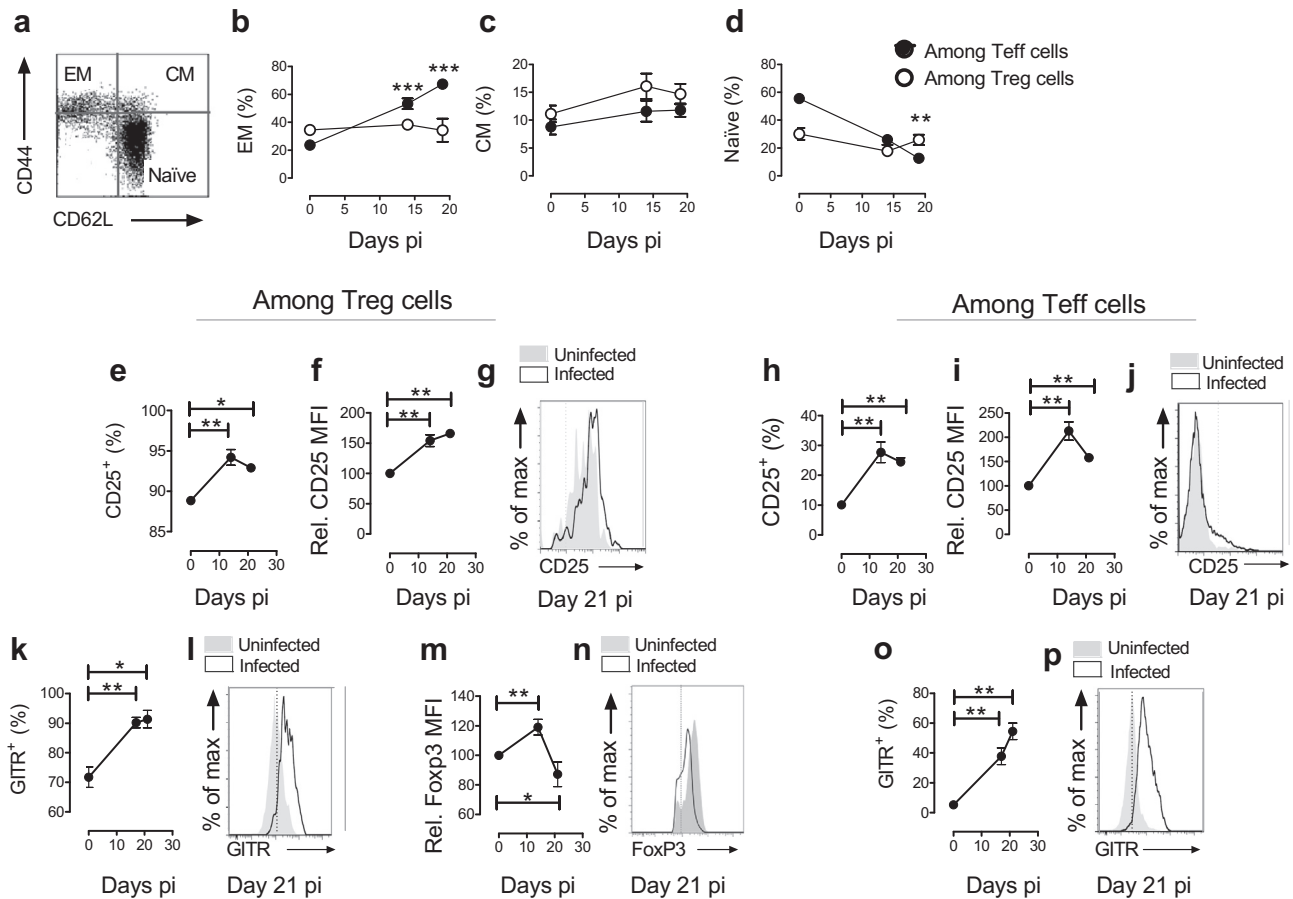
Fig. 4. Different distribution of naïve and effector phenotypes is observed between Treg and Teff cells. Spleens were obtained after 0, 14 and 9 days pi and splenocytes were stained with anti-CD44, anti-CD62L, anti-CD4 and anti-Foxp3 antibodies. (a) Dot plot illustrate CD44 and CD62L staining profiles of Treg (CD4$^+$Foxp3$^+$) cells and Teff (CD4$^+$Foxp3$^-$) cells, defined naïve, central memory (CM) and effector memory (EM) cells as CD62L^{hi}CD44^{low}, CD62L^{hi}CD44^{hi}, and CD62L^{low}CD44^{hi}, respectively. Comparative analysis of: (b) EM; (c) CM; and (d) naïve cells proportions between Treg cells (open circles) and Teff cells (closed circles) during infection by flow cytometry (n = 3–5/group/day). Results shown are representative of two independent experimental rounds. Differences between Treg and Teff cells at the same day pi: $^{**}p < 0.01$ and $^{***}p < 0.005$. (e) CD25 frequency; (f) CD25 relative MFI; and (g) representative histogram of CD25 expression among Treg (CD4$^+$Foxp3$^+$) cells in infected and uninfected mice. (h) CD25 frequency; (i) CD25 relative MFI; and (j) representative histograms of CD25 expression among Teff (CD4$^+$Foxp3$^-$) cells in infected and uninfected mice. (k) GITR frequency; and (l) representative histogram of GITR expression among Treg (CD4$^+$Foxp3$^+$) cells in infected and uninfected mice. (m) Foxp3 relative MFI among Treg (CD4$^+$Foxp3$^+$) cells after 14 and 21 days pi. The values are normalized to MFI obtained in uninfected animals. (n) Histogram representing Foxp3 expression among Treg cells in infected and uninfected mice after 21 days pi. (o) GITR frequency, and (p) representative histogram of GITR expression among Teff (CD4$^+$Foxp3$^-$) cells in infected and uninfected mice. Results shown are representative at least three independent experimental rounds (n = 3–6/group/day). Differences respect to day 0 pi: $^*p < 0.05$ and $^{**}p < 0.01$.

Smigiel et al., 2014). Accordingly, cells with a central memory profile recirculate through secondary lymphoid tissues, whereas cells with an effector memory profile recirculate predominantly among non-lymphoid tissues. To study the effector- or memory-like profile acquired by T cells during disease, we defined naïve, central memory (CM) and effector memory (EM) cells as CD62L^{hi}CD44^{low}, CD62L^{hi}CD44^{hi}, and CD62L^{low}CD44^{hi}, respectively as shown in Fig. 4a. In the spleen, a significant increase in the proportion of Teff cells with an effector memory phenotype was observed at 14 days pi, which was paralleled by a diminution of naïve cells (Fig. 4b and c). In contrast, EM Treg cells diminished significantly, while the naïve ones diminished slightly at day 14 pi and afterwards tended to keep within the same level (Fig. 4b and c). Along infection, CM cells showed similar proportions between Treg and Teff cells (Fig. 4d). Consequently, in the spleen, Teff cells showed a more strong capacity to turn into an effector phenotype than Treg cells, during infection.

We also studied the expression of CD25 (IL-2Rα-chain) and GITR, which are markers of T cell activation. After infection, CD25 expression increased from ∼88% to ∼93% on Treg cells (Fig. 4e), and from ∼10% to ∼27% on Teff cells (Fig. 4h). This was accompanied by a significant increase in CD25 MFI in both T cell

subpopulations: ∼160% in Treg cells (Fig. 4f and g) and ∼175% in Teff cells (Fig. 4i and j) as the infection progressed. Also, the proportions of GITR$^+$ Treg and Teff cells increased along the acute phase, underlying a higher activation state in both subpopulations, showing values of ∼90% in Treg cells (Fig. 4k and l) and of 60% in Teff cells at day 21 pi (Fig. 4o and p). Of note, the MFI of Foxp3 in splenic Treg cells significantly increased by day14 pi. Remarkably, at day 21 pi, the MFI of Foxp3 was drastically decreased to levels even lower than the basal ones (Fig. 4m and n). Similar tendencies were observed in dLN and blood (*data not shown*). Collectively, these data indicated that although Treg cells show signs of activation, namely increased CD25 and GITR expression, they remain mainly in a naïve state and loose Foxp3 expression level, which could be at the root of impaired Treg cell function.

3.5. T. cruzi infection induces the expression of IFN-γ and T-bet by Treg cells

Recent reports showed that Treg cells can be influenced by inflammatory factors and, in consequence, acquire the expression of distinct transcription factors and cytokine production affecting the regulatory response (Sakaguchi et al., 2013). At the same time,
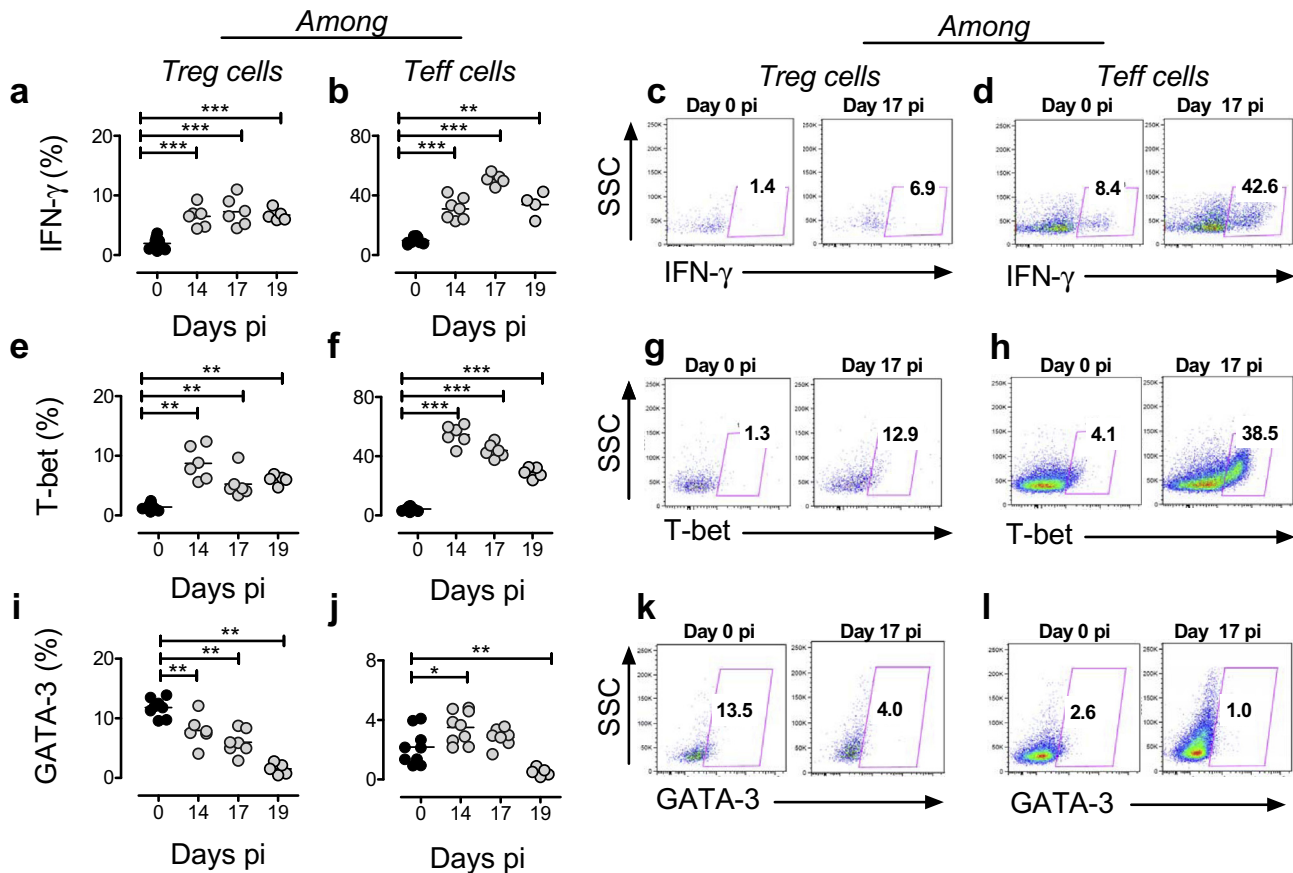
Fig. 5. *T. cruzi* infection induces the expression of IFN-γ and T-bet by Treg cells. Mice were sacrificed after 0, 14, 17 and 19 days pi, splenocytes were obtained and shortly stimulated *in vitro* with PMA plus ionomycin in the presence of brefeldin A and afterwards stained for CD4, Foxp3, IFN-γ, T-bet and GATA-3. Graphs showed the percentage of IFN-γ production among splenic Treg (a) and Teff cells (b); and representative dot plots illustrate IFN-γ intracellular staining profiles among both populations (c and d). Frequency of T-bet production among splenic Treg (e) and Teff cells (f); and representative dot plots exemplify T-bet intracellular staining profiles among both populations (g and h). Frequency of GATA-3 production among splenic Treg (i) and Teff cells (j); and representative dot plots show GATA-3 intracellular staining profiles among both populations (k-l). Each dot plot represents one mouse and numbers inside quadrants indicate the percentage of cytokine-staining cells recorded in each subpopulation. The results shown are data from two cumulate independent experiments, where circles represent individual mice and horizontal bars are the means (*n* = 4–10/group/day). *p < 0.05, **p < 0.01 and ***p < 0.005 vs. day 0.
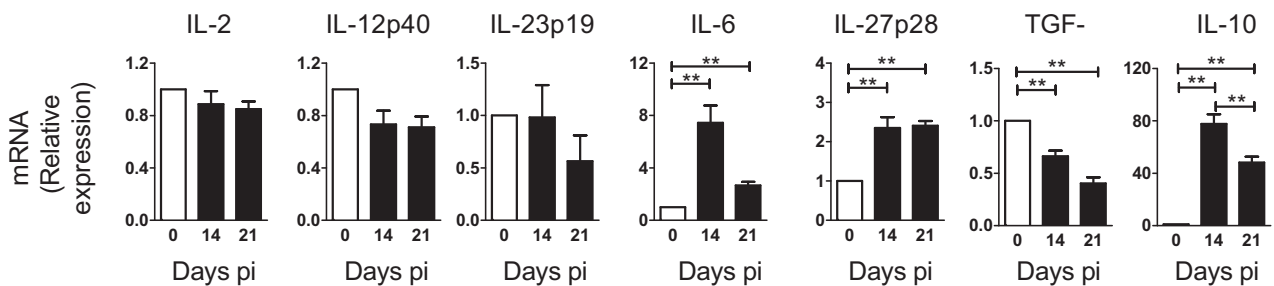

Fig. 6. *T. cruzi* infection induces an enrichment of IL-27p28 splenic transcripts. After, 0, 14 and 21 days pi, mRNA was extracted from splenocytes and quantitative real time RT-PCR of IL-2, IL-12p40, IL-23p19, IL-6, IL-27p28, TGF-β, IL-10 mRNA was performed. Bars show the relative expression of each splenic transcript by mg of tissue (*n* = 3–6/day). Representative results of two independent experiments (*n* = 3–6/group/day). *p < 0.05 and **p < 0.01 vs. day 0.

the same factors might favor the Teff cell response. Since Th1, Th2 and Th17 responses contribute to an effective anti-*T. cruzi* response, we assessed the production of IFN-γ, IL-4, IL-10 and IL-17 by splenic Treg and Teff cells and the expression of their associated canonical transcription factors: T-bet, GATA-3 and ROR-γt. Albeit to a lower proportion than Teff cells, during infection Treg cells also acquired a Th1-like polarized pattern, as indicated by the detection of IFN-γ production (Fig. 5a and c) and T-bet induction (Fig. 5e and g). As expected, infected animals showed an important proportion of IFN-γ-expressing Teff cells (Fig. 5b and d) paralleled to a strong

up-regulation of T-bet expression (Fig. 5f and h). Th17 profile analysis showed that only a low proportion of CD4⁺ Teff and Treg cells synthetized IL-17 and expressed ROR-γt in uninfected animals and both became undetectable after infection (*data not shown*). Additionally, Treg and Teff cells showed no detectable levels of IL-4 or IL-10 expression (*data not shown*) which might be explained by the strongly down-regulation of GATA-3 expression along infection (Fig. 5i–l). Likewise, GATA-3 basal expression in Treg cells was ~3-fold times higher than the observed in Teff cells, and both gradually diminished till near undetectable levels by day 19 pi
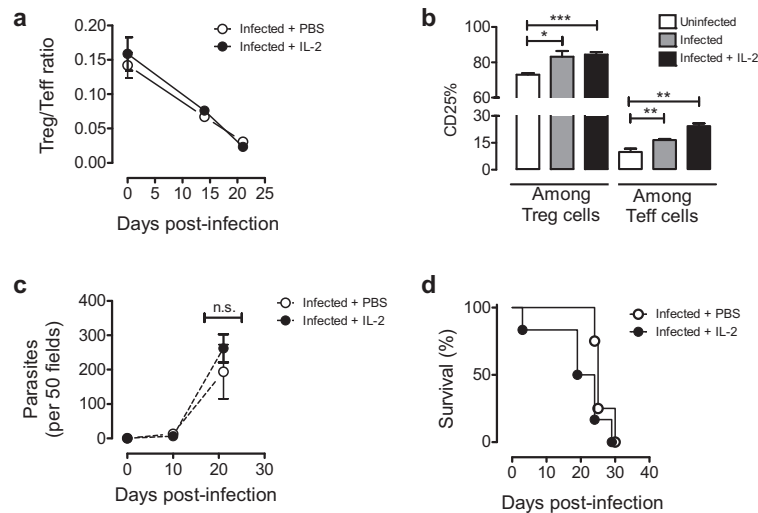
Fig. 7. IL-2 treatment during infection fails to improve Treg cells response Low doses of IL-2 (50,000 U) or PBS were administrated diary during the first 10 days pi (*n* = 5–8/group/day). (a) Treg/Teff ratio along infection. (b) Frequency of CD25 expression in Tregs and Teff cells after 21 days pi. (c) Blood parasite burden in IL-2 or PBS treated and infected mice. (d) Survival curve of IL-2 or PBS treated and infected mice. Results are representative of two independent experiments. $^{*}p$ < 0.05, $^{**}p$ < 0.01 and $^{***}p$ < 0.001 vs. uninfected mice.

(Fig. 5i). These results show that *T. cruzi*-driven inflammation promotes a Th1 effector phenotype in Teff cells but at the same time induces a skewed Th1-like profile in Treg cells.

3.6. Upon T. cruzi infection spleen cells readily produce pro- and anti-inflammatory cytokines transcripts, notably IL-27p28

Lymphoid organ microenvironment influences the development and polarization of T cells. IL-2 is the more evident key player in the promotion of Treg cell expansion and survival, but other cytokines may also influence Treg cell fate and their Th-like profile, like IL-12 cytokine family members (IL-23 and IL-27) and IL-6 among many others (La Cava, 2008). While IL-23 seems to be involved in the development of the Th17 response, IL-12 and IL-27 are involved in the development of the Th1-like phenotype by up-regulating the expression of the transcription factor T-bet in T cells (Yoshimoto et al., 2007). Thus, to evaluate the inflammatory *milieu* during *T. cruzi* infection, splenic cells obtained along different time points upon infection were *ex vivo* stimulated with PMA/ionomycin and assayed for IL-2, IL-6, IL-12p40, IL-23p19, IL-27p28, IL-10 and TGF-β mRNA expression levels by RT-qPCR. As seen in Fig. 6, splenic IL-2, IL-12p40 and IL-23p19 transcript levels remained unchanged along the whole experimental procedure. IL-6 mRNA levels peaked by day 14 pi and dropped to near basal levels by day 21 pi. Strikingly, IL-27p28 mRNA expression was clearly up-regulated all along the infection. TGF-β was progressively reduced upon infection, while IL-10, which was undetectable in uninfected animals, increased by day 14 pi and slightly decreased by day 21 pi. Of note, in this model *T. cruzi* infection reproducibly induces an important splenomegaly as a consequence of the strong immune activation, as illustrated in Supplementary Fig. 1a. Consequently, when we weight-adjusted transcript levels to mg of splenic tissue, we observed that all mRNA analyzed are increased during the infection (Supplementary Fig. 1b). The most strikingly results were observed for IL-27p28, which mRNA levels increased both at relative and at tissue expression levels, suggesting that IL-27 could contribute to shape the T cell fate during acute infection.

3.7. Low-dose IL-2 administration fails to control acute T. cruzi infection

We have previously shown that administration of low doses of IL-2 specifically boosts Treg cells, contributing to the control of inflammation and the induction of autoimmune diabetes reversal in NOD mice (Grinberg-Bleyer et al., 2010; Tang et al., 2008; Baeyens et al., 2013). Thus, we tested a similar strategy to boost Treg cells early during *T. cruzi* infection. IL-2 treatment of uninfected mice during 10 consecutive days, induced a ~2 time increase of blood Treg cells (untreated mice: 4.6 ± 0.9; IL-2 treated mice: 9.4 ± 1.2; *p* < 0.05). However, low-dose IL-2 administration during the first 5 or 10 days of infection failed to increase the percentage or absolute number of Treg cells (*not shown*) and the Treg/Teff ratio was similar in IL-2-treated and untreated mice (Fig. 7a). Interestingly, in infected animals treated with IL-2, there was a significant increase not only in the proportion of CD25^{+} Treg cells, but also in CD25^{+}Teff cells, suggesting that upon *T. cruzi* challenge low-dose IL-2 treatment loses specificity for Treg cells. Indeed, the administration of low-dose IL-2 mainly activated Teff cells, since at day 21 pi the increment of CD25^{+} T cells was of ~47% and ~10% in Teff and Treg cells, respectively (Fig. 7b). This failure of low-dose IL-2 therapy to specifically boost Treg cells was associated with no changes in the course of infection as attested by unchanged parasitemia (Fig. 7c) and mice survival (Fig. 7d).

3.8. IL-2 plus Dexamethasone combined treatment improves the survival of infected mice, in part by modifying the Th1/Th2 balance

It has been previously reported that Dex suppresses the activation of Teff cells and can amplify the IL-2-dependent Treg cell expansion (Xie et al., 2009). Thus, we hypothesized that Dex could synergize with low-doses of IL-2 to boost endogenous Treg cells and improve *T. cruzi* infection. To that end, we first compared the impact of the administration of IL-2, Dex alone or the combined treatment (IL-2 + Dex) on Treg cells in uninfected C57BL/6 mice. As shown in Fig. 8a, all treatments increased blood Treg cell frequencies by day 7, being Dex and IL-2 + Dex effects significantly
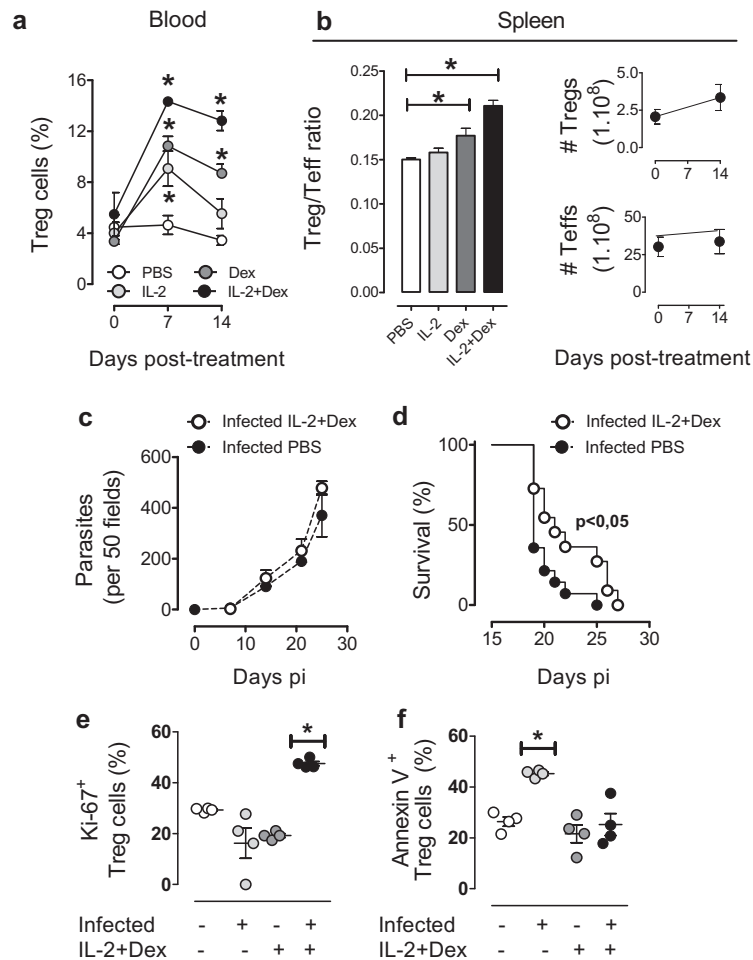
Fig. 8. IL-2 plus dexamethasone combined treatment improves the survival of *T. cruzi* infected mice. First, mice were treated with IL-2, Dex alone or the combined treatment (IL-2 + Dex) during 7 consecutive days. Comparative studies showing the impact of IL-2, Dex alone or the combined IL-2 + Dex administration on: (a) blood Treg cells frequency in uninfected C57BL/6 mice 7 and 14 days post-treatment; and (b) Treg/Teff ratio (left panel) and absolute number of Treg cells and Teff cells (right panel) after 14 days post-treatment. Representative results of two independent experiments (*n* = 4–6/group). *$p < 0.05$ vs. uninfected mice. Second, mice received a prophylactic treatment combining IL-2 + Dex during 7 days before infection. (c) Blood parasite burden in C57BL/6 mice pre-treated with IL-2 + Dex combined treatment compared to non-treated and infected animals; and (d) representative survival curve (*n* = 8/group). Impact of combined treatment after 14 days post-infection upon: (e) Ki-67⁺ Treg cells frequency and (f) annexin V⁺ percentage among Tregs. Representative results of two independent experiments (*n* = 4/group). *$p < 0.05$ compared to the rest groups.

higher and longer lasting. Also, in the spleen, upon Dex and IL-2 + Dex administration, Treg/Teff ratio remained elevated for at least up to 14 days (Fig. 8b, left panel), being the combined treatment the most effective. In addition, IL-2 + Dex administration, increase the absolute number of Treg cells (Fig. 8b, right panel). Thus, considering the synergistic effect of the combined treatment to boost Treg cells in uninfected animals we tested the therapeutic potential of this treatment when administered in a prophylactic schedule, beginning 7 days before infection. Although this treatment did not modify the parasitemia (Fig. 8c), it significantly increased mice survival time ($p < 0.05$; Fig. 8d) demonstrating a better control of inflammation. Of note, Treg cells from IL-2 + Dex treated and infected mice displayed enhanced proliferation 14 days after infection, as indicated by the significant increased percentage of Ki-67⁺ Treg cells (Fig. 8e) and lower cell death (Fig. 8f) in treated animals compared to the others groups. These results indicate that IL-2 + Dex treatment favors the expansion and survival of Treg cells exposed to the *T. cruzi*-induced inflammatory environment. To evaluate if these changes were associated with differential Th-polarization patterns of Treg cells and Teff cells during infection, we next assessed the expression levels of T-bet, ROR-γt, GATA-3, IFN-γ, IL-17, IL-4 and IL-10 in both populations. Interestingly, IL-2 + Dex treatment was associated with an increase in IFN-γ production and T-bet expression by Treg and Teff

cells from IL-2 + Dex treated and infected mice (Fig. 9a and b, respectively). Notably, the combined treatment also induced the expression of GATA-3 (Fig. 9c) and the appearance of a small proportion of Treg cells producing IL-4 and IL-10 (~2.5% and ~4%, respectively). Similar results were observed in Teff cells (*data not shown*). It is remarkable that by day 14pi, ~40% of the Treg cells of IL-2 + Dex pre-treated mice were GATA-3⁺, compared to only ~6% of the Teff cells.

We also compared the transcript levels of IL-2, IL-6, IL-12p40, IL-23p19, IL-27p28, IL-10 and TGF-β in the spleen of infected mice, pre-treated or not, and observed no major modifications in the tested cytokines (*data not shown*), except for an enhancement of mRNA expression of IL-27p28 and IL-10 (Fig. 9d left and right panels, respectively), although at low levels. Overall, our data suggest that the combined therapy with IL-2 + Dex allows the emergence of GATA-3 expression on T cells and modulates the systemic cytokine production, which may be viewed as a more balanced immune response, reflected in the increased survival time of the infected mice.

4. Discussion

The degree to which *T. cruzi* is capable of causing immunopathology is dependent on the mouse genetic background and the
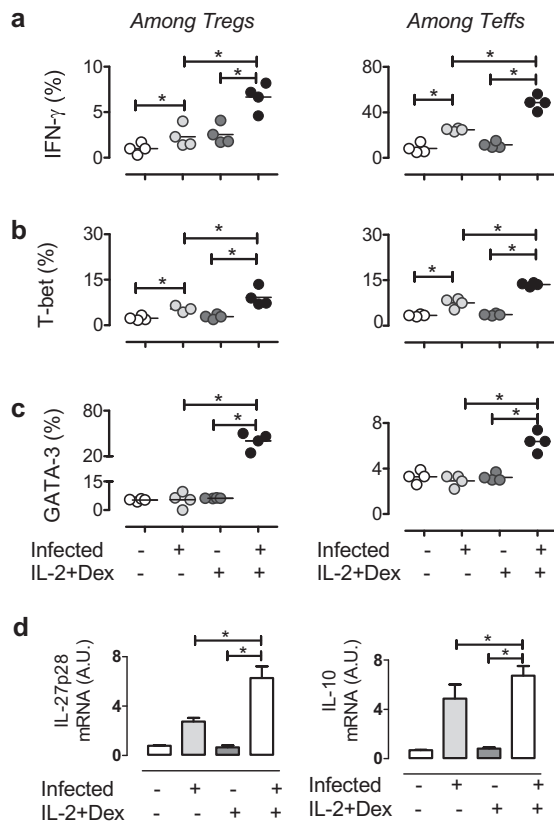
Fig. 9. IL-2 + Dex treatment was associated with an increase in T-bet expression and IFN-γ production in infected mice. Mice pre-treated with IL-2 + Dex were infected and sacrificed after 14 days pi, splenocytes were obtained and shortly stimulated *in vitro* with PMA plus ionomycin in the presence of brefeldin A and afterwards stained for CD4, Foxp3, IFN-γ, T-bet and GATA-3. (a) Graphs showed the percentage of IFN-γ production among splenic Treg and Teff cells; (b) frequency of T-bet production among splenic Treg and Teff cells; (c) frequency of GATA-3 production among splenic Treg and Teff cells; and representative dot plots showing GATA-3 intracellular staining profiles among both populations; and (d) mRNA expression of IL-27p28 and IL-10 (left and right panels, respectively). Results shown are data from two independent experiments, where circles represent individual mice and horizontal bars are the means (n = 4/group). $^{*}p < 0.05$, $^{**}p < 0.01$ and $^{***}p < 0.005$ vs. day 0.

and targets specific sequences called glucocorticoid response elements (GREs) in the promoter regions of glucocorticoid-inducible genes (Vandevyver et al., 2013). Thus, Treg and Teff cells might differ in the level of glucocorticoid receptor expression and in the number of GREs, and in addition, the promoter region of Foxp3 gene expression might be under the positive control of GREs (transactivation), favoring the Treg cell expansion and suppressor function. In addition, glucocorticoids can also modulate gene expression via trans repression, a mechanism largely based on protein:protein interactions (Ratman et al., 2013), which could differ between Treg and Teff cells. However, these possibilities have not yet been investigated.

Besides a number of reports showed a positive effect of glucocorticoids upon Treg cells, some opposed data were obtained in human and mice models. These conflicted data could be caused by dissimilarities in the doses and timing of glucocorticoid administration, variances in the characterization of Treg cells (CD25^{+} Foxp3^{+}, CD4^{+}CD25^{high}, CD25^{+}Foxp3^{+}, etc) and also intrinsic differences in the immunological background of studied diseases (Chen et al., 2006; Wüst et al., 2008; Karagiannidis et al., 2004; Azab et al., 2008; Sbiera et al., 2011; Pandolfi et al., 2013). Of note, these studies were carried out mainly in autoimmune backgrounds and might profoundly differ from an infectious condition. In our hands, the endogenous levels of corticosterone appear to preferentially affect Teff than Treg cells. It is plausible that, besides glucocorticoids, other adrenal hormones could influence Treg/Teff cell homeostasis and cytokine profile during *T. cruzi* infection. In accordance, it has been proposed that the timing of glucocorticoid response and the levels of anti-glucocorticoid hormones like DHEA could affect the cellular response and the course of experimental tuberculosis (Hernandez-Pando et al., 1998).

In the context of acute *T. cruzi* infection, the failure of Treg function seems to be related to complex mechanisms. Interleukin-2 is the more prominent cytokine involved in the expansion and survival of peripheral Treg cells (Fontenot et al., 2005a,b). Nevertheless, the incapacity of splenic Treg cells to expand, proliferate and activate during this parasitic infection does not appear to be dependent on the bioavailability of IL-2, since splenic IL-2 mRNA levels are preserved along infection. Moreover, IL-2 supplementation at low doses during the course of disease fails to increase Treg cell numbers. However, we cannot rule out the fact that deprivation of other essential factors may be affecting the expansion of Treg cells.

The increase in the proportion of CD44^{high} EM or CM T cells during inflammation is known to result from naïve cell activation in secondary lymphoid organs (Huehn et al., 2004). In our experimental model of *T. cruzi* infection, we observed a significant increase in the proportion of Teff cells with EM phenotype at the expense of a diminution in the proportion of Treg cells with this phenotype, clearly highlighting that in this extremely inflammatory *milieu*, Treg cells are less efficient than Teff cells to get activated. This striking observation may result from either a Treg cell-specific sensitivity to inflammatory cues or to a relative lower frequency of *T. cruzi* specific-Treg cells compared to Teff cells. In addition, this profile might affect the proper homing of EM Tregs to peripheral organs, necessary to cope with inflammation. Of note, it has been previously shown that an inflammatory environment characterized by increased systemic levels of TNF-α, IL-6, IL-1β is rapidly installed upon *T. cruzi* infection in C57BL/6 mice (Perez et al., 2007; Roggero et al., 2002), and accompanied by a delayed production of anti-inflammatory mediators. Expanding these observations we now document an early systemic increase of IFN-γ together with a detectable, yet delayed, production of IL-10, and increased splenic transcripts for pro- and anti-inflammatory cytokines. Since IFN-γ, TNF-α, IL-6 and IL-1β can exert inhibitory actions on Treg cells, affecting their differentiation, proliferation

dose and clones of parasites used. Thus, studies reporting the role of Treg cells in the control of infection or immunopathology are controversial, whereby the dynamic that is established between Treg and Teff cells during infection still remains unclear (Kotner and Tarleton, 2007; Sales et al., 2008). We previously demonstrated that *T. cruzi* infection in C57BL/6 mice induces an exacerbated and dysregulated Th1 pro-inflammatory response associated with lethal immunopathology, mainly because of a collapsed immune-endocrine regulatory network (Perez et al., 2007; Roggero et al., 2002, 2006). Expanding our previous findings, we show here that during infection Treg cells seem dysfunctional and overwhelmed by the Teff cell response. In addition, decreasing physiological corticosterone levels by Adx does not induce changes in Treg cell numbers. Furthermore, we demonstrated for the first time that endogenous glucocorticoids released in response to *T. cruzi*-driven immune activation are crucial to sustain the Treg/Teff ratio, reinforcing the view that besides intrinsic immunological mechanisms, inflammation is also under an endocrine control.

The beneficial effect of corticosterone upon the Treg/Teff ratio might be also related with the possibility that Treg and Teff cells differ in their sensitivity to the hormone. Is known that glucocorticoids mediate their biological effects through the binding to their cognate intracellular receptor, which translocates to the nucleus

and function (La Cava, 2008), as well as rendering Teff cells refractory to Treg cell suppression, present changes in cytokine dynamics may contribute to the failure of the regulatory response (Caretto et al., 2010; O'Sullivan et al., 2006; Valencia et al., 2006; Wan et al., 2007).

It is well described that T-bet expression is associated to IFN-γ production and to the establishment of a Th1 inflammatory *milieu*. T-bet- and IFN-γ-expressing Treg cells have been previously described in *Toxoplasma gondii* and coronavirus infections (Hall et al., 2012a; Oldenhove et al., 2009; Zhao et al., 2011). It is not surprising, therefore, that under the highly Th1-polarized microenvironment arising during *T. cruzi* infection, an emergence of T-bet and IFN-γ expressing Treg cells occurs, paralleling the acquisition of a Th1 phenotype by Teff cells (Sakaguchi et al., 2013; Koch et al., 2009). The secretion of IFN-γ during *T. cruzi* infection likely contributes to host tissue injury, activating tissue macrophages to secrete TNF-α and to damage heart and other tissues (Silverio et al., 2012). Moreover, the acquisition of this effector phenotype might favor their traffic to Th1-inflamed tissues and disturb their local suppressor function (Smigiel et al., 2014).

Differentiation of naive T cells into effector Th2 cells and the concomitant production of Th2 cytokines are controlled by the transcription factor GATA-3. Moreover, GATA-3 plays a key role in Treg cell physiology during inflammatory processes, influencing Treg accumulation in inflamed tissues and sustaining Foxp3 expression (Wohlfert et al., 2011). Here, we observed that during *T. cruzi* infection, although there is a substantial proportion of Teff cells that acquire T-bet expression, very few Teff cells become GATA-3⁺, reinforcing the view that this lethal infection is associated with a highly skewed Teff Th1-like polarization. Concerning Treg cells, the proportion of these cells expressing GATA-3 gradually diminished from ∼12% in uninfected mice to almost undetectable levels by day 19 pi. Moreover, this loss of GATA-3 expression in Treg cells was accompanied by a gain in T-bet expression and in the production of IFN-γ. Of note, these findings are associated to the scarce presence of Treg cells in *T. cruzi*-target tissues and the diminution of Foxp3 MFI. These data reminds findings from Wohlfert et al. (2011) showing that GATA-3 expressing Treg cells in inflamed settings restrict the magnitude of their self Th1-polarization and the production of inflammatory cytokines.

Nowadays, acute Chagas disease is treated by chemotherapy targeted to the parasite. However, these therapies can be toxic and fail due to diverse causes. Although in children chemotherapies are quite effective (∼57 and 71% of cure in chronic or acute phase, respectively), a substantial amount of treatment failures is seen in adults (Matta Guedes et al., 2012). Regarding Benznidazol, we and others have described that this drug not only kills the parasite but also exert immunomodulatory effects (Piaggio et al., 2001; Ronco et al., 2011). Consequently, modulating the inflammatory response associated to *T. cruzi* infection stands as a promising approach for tackling this disease. Along these lines, boosting endogenous Treg cells sounds instrumental to dampen inflammation. One strategy to activate Treg cells is the administration of low doses of IL-2 which has been shown by us and others to effectively activate Treg cells reinforcing their suppressive function and contributing to the control chronic inflammation and autoimmunity in mice (Tang et al., 2008; Webster et al., 2009; Wilson et al., 2008; Dinh et al., 2012) and humans (Koreth et al., 2011; Saadoun et al., 2011). Particularly, we showed that low-dose IL-2 administration to pre-diabetic NOD mice which prevents disease development, increases Treg proportions specifically in the pancreas and these IL-2 expanded Treg cells express higher levels of Bcl-2, CD25, and Foxp3, suggestive of increased resistance to apoptosis and higher activation (Tang et al., 2008; Grinberg-Bleyer et al., 2010). Here, we administered for the first time low doses of IL-2 during *T. cruzi* infection. However, IL-2 doses similar to the ones

successfully used to treat type 1 diabetes (Grinberg-Bleyer et al., 2010) did not show any noticeable effect on parasitemia and immunopathology. This lack of efficacy of IL-2 treatment can be explained by the fact that upon *T. cruzi* infection, Teff cells rapidly up-regulate CD25 and consequently become highly sensitive to low doses of IL-2, being the IL-2-specific effect on Treg cells lost.

An alternative way to activate Treg cells may be to use synthetic glucocorticoids in combination with IL-2 (Barrat et al., 2002; Unger et al., 2009), particularly when taking into account our previous results wherein endogenous glucocorticoids are necessary for sustaining a balanced Treg/Teff response during acute *T. cruzi* infection, and that Dex supplementation expanded IL-2-driven Treg cell development in an acute model of GVHD (Xie et al., 2009). Thus, we first studied the effect of these drugs on Treg cells in untreated mice, and observed synergistic effects of the combined treatment. Consequently, we tested the modulatory potential of combined IL-2 + Dex pre-treatment on *T. cruzi* infection. We showed that Dex + IL-2 combined therapy improved Treg cell proliferation and survival and favors Treg/Teff ratio; in addition to inducing Treg GATA-3 expression and IL-4 and IL-10 production during infection, suggesting a better immune balance. Moreover, an increase in mouse survival time, in our highly lethal model of *T. cruzi* infection was observed upon combined treatment with Dex + IL-2. These findings were associated with a splenic microenvironment enriched in IL-10 and IL-27p28 transcript levels. Along these lines, Hall and collaborators showed that during *T. gondii* infection, IL-27 improved T-bet expression and enhanced IL-10 secretion by Treg cells, enhancing their Th1-suppressor capacity (Hall et al., 2012a). Moreover, IL-27 can promote IL-10 production by Teff cells (Hall et al., 2012b). Thus, besides the known beneficial anti-inflammatory effects that IL-10 exerts on Teff cells, IL-27 increased production might also be involved in the dampening of inflammation. In addition, besides we were unable to quantified transcripts of IL-4 in splenocytes, the fact that IL-4 expression was also detected in Treg and Teff cells after IL-2 + Dex treatment also gives a notion that combined treatment induces a more balanced Th1/Th2 response.

In summary, here we provide new insights into the physiopathology of acute *T. cruzi* infection. We show that endogenous glucocorticoids influence the Treg and Teff cell dynamics during *T. cruzi* infection, affecting mainly the Teff response. Moreover, rapidly upon infection, Treg cells acquire a typical Th-1 like pathogenic phenotype and are overwhelmed by rapidly proliferating Teff cells. Interestingly, the demonstration that administration of IL-2 + Dex modulates Treg/Teff homeostasis and influence disease outcome opens new perspectives for preventing the immunopathology associated to *T. cruzi* infection. Indeed, our results pave the way to the design of optimized therapies aimed to specifically boost Treg cells during *T. cruzi* infection, which combined with antiparasitic drugs may help to control both the parasite and the excessive pathologic inflammatory process induced by it.

Appendix A. Supplementary data

Supplementary data associated with this article can be found, in the online version, at http://dx.doi.org/10.1016/j.bbi.2014.11.016.

References

Azab, N.A., Bassyouni, I.H., Emad, Y., Abd El-Wahab, G.A., Hamdy, G., Mashahit, M.A., 2008. CD4+CD25+ regulatory T cells (TREG) in systemic lupus erythematosus (SLE) patients: the possible influence of treatment with corticosteroids. Clin. Immunol. 127, 151–157.

Bachmann, M.F., Wolint, P., Walton, S., Schwarz, K., Oxenius, A., 2007. Differential role of IL-2R signaling for CD8+ T cell responses in acute and chronic viral infections. Eur. J. Immunol. 37, 1502–1512.

Barrat, F.J., Cua, D.J., Boonstra, A., Richards, D.F., Crain, C., Savelkoul, H.F., de Waal-Malefyt, R., Coffman, R.L., Hawrylowicz, C.M., O'Garra, A., 2002. In vitro generation of interleukin 10-producing regulatory CD4(+) T cells is induced by immunosuppressive drugs and inhibited by T helper type 1 (Th1)- and Th2-inducing cytokines. J. Exp. Med. 195, 603–616.

Baeyens, A., Pérol, L., Fourcade, G., Cagnard, N., Carpentier, W., Woytschak, J., Boyman, O., Hartemann, A., Piaggio, E., 2013. Limitations of IL-2 and rapamycin in immunotherapy of type 1 diabetes. Diabetes 62 (9), 3120–3131.

Caretto, D., Katzman, S.D., Villarino, A.V., Gallo, E., Abbas, A.K., 2010. Cutting edge: the Th1 response inhibits the generation of peripheral regulatory T cells. J. Immunol. 184, 30–34.

Coura, J.R., Borges-Pereira, J., 2010. Chagas disease: 100 years after its discovery. A systemic review. Acta Trop. 115, 5–13.

Chen, X., Oppenheim, J.J., Winkler-Pickett, R.T., Ortaldo, J.R., Howard, O.M., 2006. Glucocorticoid amplifies IL-2-dependent expansion of functional FoxP3(+)CD4(+)CD25(+) T regulatory cells in vivo and enhances their capacity to suppress EAE. Eur. J. Immunol. 36, 2139–2149.

de Araujo, F.F., Vitelli-Avelar, D.M., Teixeira-Carvalho, A., Antas, P.R., Assis Silva Gomes, J., Sathler-Avelar, R., Otavio Costa Rocha, M., Eloi-Santos, S.M., Pinho, R.T., Correa-Oliveira, R., Martins-Filho, O.A., 2011. Regulatory T cells phenotype in different clinical forms of Chagas' disease. PLoS Negl. Trop. Dis. 5, e992.

Dinh, T.N., Kyaw, T.S., Kanellakis, P., To, K., Tipping, P., Toh, B.H., Bobik, A., Agrotis, A., 2012. Cytokine therapy with interleukin-2/anti-interleukin-2 monoclonal antibody complexes expands CD4+CD25+Foxp3+ regulatory T cells and attenuates development and progression of atherosclerosis. Circulation 126, 1256–1266.

Dutra, W.O., Menezes, C.A., Magalhaes, L.M., Gollob, K.J., 2014. Immunoregulatory networks in human Chagas disease. Parasite Immunol. 36 (8), 377–387.

Dutt, S., Tseng, D., Ermann, J., George, T.I., Liu, Y.P., Davis, C.R., Fathman, C.G., Strober, S., 2007. Naive and memory T cells induce different types of graft-versus-host disease. J. Immunol. 179, 6547–6554.

Fehervari, Z., Yamaguchi, T., Sakaguchi, S., 2006. The dichotomous role of IL-2: tolerance versus immunity. Trends Immunol. 27, 109–111.

Fontenot, J.D., Dooley, J.L., Farr, A.G., Rudensky, A.Y., 2005a. Developmental regulation of Foxp3 expression during ontogeny. J. Exp. Med. 202, 901–906.

Fontenot, J.D., Rasmussen, J.P., Gavin, M.A., Rudensky, A.Y., 2005b. A function for interleukin 2 in Foxp3-expressing regulatory T cells. Nat. Immunol. 6, 1142–1151.

Grinberg-Bleyer, Y., Baeyens, A., You, S., Elhage, R., Fourcade, G., Gregoire, S., Cagnard, N., Carpentier, W., Tang, Q., Bluestone, J., Chatenoud, L., Klatzmann, D., Salomon, B.L., Piaggio, E., 2010. IL-2 reverses established type 1 diabetes in NOD mice by a local effect on pancreatic regulatory T cells. J. Exp. Med. 207, 1871–1878.

Hall, A.O., Beiting, D.P., Tato, C., John, B., Oldenhove, G., Lombana, C.G., Pritchard, G.H., Silver, J.S., Bouladoux, N., Stumhofer, J.S., Harris, T.H., Grainger, J., Wojno, E.D., Wagage, S., Roos, D.S., Scott, P., Turka, L.A., Cherry, S., Reiner, S.L., Cua, D., Belkaid, Y., Elloso, M.M., Hunter, C.A., 2012a. The cytokines interleukin 27 and interferon-gamma promote distinct Treg cell populations required to limit infection-induced pathology. Immunity 37, 511–523.

Hall, A.O., Silver, J.S., Hunter, C.A., 2012b. The immunobiology of IL-27. Adv. Immunol. 115, 1–44.

Hall, B.M., Tran, G.T., Verma, N.D., Plain, K.M., Robinson, C.M., Nomura, M., Hodgkinson, S.J., 2013. Do natural T regulatory cells become activated to antigen specific T regulatory cells in transplantation and in autoimmunity? Front. Immunol. 4, 208.

Hernandez-Pando, R., Streber, M., Orozco, H., Arriaga, K., Pavon, L., Al-Nakhli, S.A., Rook, G.A., 1998. The effects of androstenediol and dehydroepiandrosterone on the course and cytokine profile of tuberculosis in BALB/c mice. Immunology 95, 234–241.

Huehn, J., Siegmund, K., Lehmann, J.C., Siewert, C., Haubold, U., Feuerer, M., Debes, G.F., Lauber, J., Frey, O., Przybylski, G.K., Niesner, U., de la Rosa, M., Schmidt, C.A., Brauer, R., Buer, J., Scheffold, A., Hamann, A., 2004. Developmental stage, phenotype, and migration distinguish naive- and effector/memory-like CD4+ regulatory T cells. J. Exp. Med. 199, 303–313.

Karagiannidis, C., Akdis, M., Holopainen, P., Woolley, N.J., Hense, G., Rückert, B., Mantel, P.Y., Menz, G., Akdis, C.A., Blaser, K., Schmidt-Weber, C.B., 2004. Glucocorticoids upregulate FOXP3 expression and regulatory T cells in asthma. J. Allergy Clin. Immunol. 114 (6), 1425–1433.

Koch, M.A., Tucker-Heard, G., Perdue, N.R., Killebrew, J.R., Urdahl, K.B., Campbell, D.J., 2009. The transcription factor T-bet controls regulatory T cell homeostasis and function during type 1 inflammation. Nat. Immunol. 10, 595–602.

Koreth, J., Matsuoka, K., Kim, H.T., McDonough, S.M., Bindra, B., Alyea 3rd, E.P., Armand, P., Cutler, C., Ho, V.T., Treister, N.S., Bienfang, D.C., Prasad, S., Tzachanis, D., Joyce, R.M., Avigan, D.E., Antin, J.H., Ritz, J., Soiffer, R.J., 2011. Interleukin-2 and regulatory T cells in graft-versus-host disease. N. Engl. J. Med. 365, 2055–2066.

Kotner, J., Tarleton, R., 2007. Endogenous CD4(+) CD25(+) regulatory T cells have a limited role in the control of Trypanosoma cruzi infection in mice. Infect. Immun. 75, 861–869.

La Cava, A., 2008. Tregs are regulated by cytokines: implications for autoimmunity. Autoimmun. Rev. 8, 83–87.

Malek, T.R., 2003. The main function of IL-2 is to promote the development of T regulatory cells. J. Leukoc. Biol. 74, 961–965.

Malek, T.R., Bayer, A.L., 2004. Tolerance, not immunity, crucially depends on IL-2. Nat. Rev. Immunol. 4, 665–674.

Mariano, F.S., Gutierrez, F.R., Pavanelli, W.R., Milanezi, C.M., Cavassani, K.A., Moreira, A.P., Ferreira, B.R., Cunha, F.Q., Cardoso, C.R., Silva, J.S., 2008. The involvement of CD4+CD25+ T cells in the acute phase of Trypanosoma cruzi infection. Microbes Infect. 10, 825–833.

Matsuoka, K., Koreth, J., Kim, H.T., Bascug, G., McDonough, S., Kawano, Y., Murase, K., Cutler, C., Ho, V.T., Alyea, E.P., Armand, P., Blazar, B.R., Antin, J.H., Soiffer, R.J., Ritz, J., 2013. Low-dose interleukin-2 therapy restores regulatory T cell homeostasis in patients with chronic graft-versus-host disease. Sci. Transl. Med. 5, 179ra143.

Matta Guedes, P.M., Gutierrez, F.R., Nascimento, M.S., Do-Valle-Matta, M.A., Silva, J.S., 2012. Antiparasitical chemotherapy in Chagas' disease cardiomyopathy: current evidence. Trop. Med. Int. Health 17, 1057–1065.

Nunes, M.C., Dones, W., Morillo, C.A., Encina, J.J., Ribeiro, A.L., Ribeiro, A.L., Council on Chagas Disease of the Interamerican Society of Cardiology, 2013. Chagas disease: an overview of clinical and epidemiological aspects. J. Am. Coll. Cardiol. 62, 767–776.

O'Sullivan, B.J., Thomas, H.E., Pai, S., Santamaria, P., Iwakura, Y., Steptoe, R.J., Kay, T.W., Thomas, R., 2006. IL-1 beta breaks tolerance through expansion of CD25+ effector T cells. J. Immunol. 176, 7278–7287.

Oldenhove, G., Bouladoux, N., Wohlfert, E.A., Hall, J.A., Chou, D., Dos Santos, L., O'Brien, S., Blank, R., Lamb, E., Natarajan, S., Kastenmayer, R., Hunter, C., Grigg, M.E., Belkaid, Y., 2009. Decrease of Foxp3+ Treg cell number and acquisition of effector cell phenotype during lethal infection. Immunity 31, 772–786.

Pandolfi, J., Baz, P., Fernández, P., Discianni Lupi, A., Payaslián, F., Billordo, L.A., Fainboim, L., Arruvito, L., 2013. Regulatory and effector T-cells are differentially modulated by Dexamethasone. Clin. Immunol. 149 (3), 400–410.

Perez, A.R., Roggero, E., Nicora, A., Palazzi, J., Besedovsky, H.O., Del Rey, A., Bottasso, O.A., 2007. Thymus atrophy during Trypanosoma cruzi infection is caused by an immuno-endocrine imbalance. Brain Behav. Immun. 21, 890–900.

Piaggio, E., Sanceau, J., Revelli, S., Bottasso, O., Wietzerbin, J., Serra, E., 2001. Trypanocidal drug benznidazole impairs lipopolysaccharide induction of macrophage nitric oxide synthase gene transcription through inhibition of NF-kappaB activation. J. Immunol. 167, 3422–3426.

Ramirez, J.D., Montilla, M., Cucunuba, Z.M., Florez, A.C., Zambrano, P., Guhl, F., 2013. Molecular epidemiology of human oral Chagas disease outbreaks in Colombia. PLoS Negl. Trop. Dis. 7, e2041.

Ratman, D., Vanden Berghe, W., Dejager, L., Libert, C., Tavernier, J., Beck, I.M., de Bosscher, K., 2013. How glucocorticoid receptors modulate the activity of other transcription factors: a scope beyond tethering. Mol. Cell. Endocrinol. 380 (1–2), 41–54.

Roggero, E., Perez, A., Tamae-Kakazu, M., Piazzon, I., Nepomnaschy, I., Wietzerbin, J., Serra, E., Revelli, S., Bottasso, O., 2002. Differential susceptibility to acute Trypanosoma cruzi infection in BALB/c and C57BL/6 mice is not associated with a distinct parasite load but cytokine abnormalities. Clin. Exp. Immunol. 128, 421–428.

Roggero, E., Perez, A.R., Bottasso, O.A., Besedovsky, H.O., Del Rey, A., 2009. Neuroendocrine-immunology of experimental Chagas' disease. Ann. N. Y. Acad. Sci. 1153, 264–271.

Roggero, E., Perez, A.R., Tamae-Kakazu, M., Piazzon, I., Nepomnaschy, I., Besedovsky, H.O., Bottasso, O.A., del Rey, A., 2006. Endogenous glucocorticoids cause thymus atrophy but are protective during acute Trypanosoma cruzi infection. J. Endocrinol. 190, 495–503.

Ronco, M.T., Manarin, R., Frances, D., Serra, E., Revelli, S., Carnovale, C., 2011. Benznidazole treatment attenuates liver NF-kappaB activity and MAPK in a cecal ligation and puncture model of sepsis. Mol. Immunol. 48, 867–873.

Saadoun, D., Rosenzwajg, M., Joly, F., Six, A., Carrat, F., Thibault, V., Sene, D., Cacoub, P., Klatzmann, D., 2011. Regulatory T-cell responses to low-dose interleukin-2 in HCV-induced vasculitis. N. Engl. J. Med. 365, 2067–2077.

Sakaguchi, S., Vignali, D.A., Rudensky, A.Y., Niec, R.E., Waldmann, H., 2013. The plasticity and stability of regulatory T cells. Nat. Rev. Immunol. 13, 461–467.

Sales Jr., P.A., Golgher, D., Oliveira, R.V., Vieira, V., Arantes, R.M., Lannes-Vieira, J., Gazzinelli, R.T., 2008. The regulatory CD4+CD25+ T cells have a limited role on pathogenesis of infection with Trypanosoma cruzi. Microbes Infect. 10, 680–688.

Sallusto, F., Lenig, D., Forster, R., Lipp, M., Lanzavecchia, A., 1999. Two subsets of memory T lymphocytes with distinct homing potentials and effector functions. Nature 401, 708–712.

Sathler-Avelar, R., Vitelli-Avelar, D.M., Teixeira-Carvalho, A., Martins-Filho, O.A., 2009. Innate immunity and regulatory T-cells in human Chagas disease: what must be understood? Mem. Inst. Oswaldo Cruz 104 (Suppl. 1), 246–251.

Savino, W., Villa-Verde, D.M., Mendes-da-Cruz, D.A., Silva-Monteiro, E., Perez, A.R., Aoki Mdel, P., Bottasso, O., Guinazu, N., Silva-Barbosa, S.D., Gea, S., 2007. Cytokines and cell adhesion receptors in the regulation of immunity to Trypanosoma cruzi. Cytokine Growth Factor Rev. 18, 107–124.

Sbiera, S., Dexneit, T., Reichardt, S.D., Michel, K.D., van den Brandt, J., Schmull, S., Kraus, L., Beyer, M., Mlynski, R., Wortmann, S., Allolio, B., Reichardt, H.M., Fassnacht, M., 2011. Influence of short-term glucocorticoid therapy on regulatory T cells in vivo. PLoS ONE 6 (9), e24345.

Silverio, J.C., Pereira, I.R., Cipitelli Mda, C., Vinagre, N.F., Rodrigues, M.M., Gazzinelli, R.T., Lannes-Vieira, J., 2012. CD8+ T-cells expressing interferon gamma or perforin play antagonistic roles in heart injury in experimental *Trypanosoma cruzi*-elicited cardiomyopathy. PLoS Pathog. 8, e1002645.

Smigiel, K.S., Richards, E., Srivastava, S., Thomas, K.R., Dudda, J.C., Klonowski, K.D., Campbell, D.J., 2014. CCR7 provides localized access to IL-2 and defines homeostatically distinct regulatory T cell subsets. J. Exp. Med. 211, 121–136.

Tang, Q., Adams, J.Y., Penaranda, C., Melli, K., Piaggio, E., Sgouroudis, E., Piccirillo, C.A., Salomon, B.L., Bluestone, J.A., 2008. Central role of defective interleukin-2 production in the triggering of islet autoimmune destruction. Immunity 28, 687–697.

Unger, W.W., Laban, S., Kleijwegt, F.S., van der Slik, A.R., Roep, B.O., 2009. Induction of Treg by monocyte-derived DC modulated by vitamin D3 or dexamethasone: differential role for PD-L1. Eur. J. Immunol. 39, 3147–3159.

Valencia, X., Stephens, G., Goldbach-Mansky, R., Wilson, M., Shevach, E.M., Lipsky, P.E., 2006. TNF downmodulates the function of human $CD4^+CD25^{hi}$ T-regulatory cells. Blood 108, 253–261.

Vandevyver, S., Dejager, L., Tuckermann, J., Libert, C., 2013. New insights into the anti-inflammatory mechanisms of glucocorticoids: an emerging role for glucocorticoid-receptor-mediated transactivation. Endocrinology 154 (3), 993–1007.

Wan, S., Xia, C., Morel, L., 2007. IL-6 produced by dendritic cells from lupus-prone mice inhibits CD4+CD25+ T cell regulatory functions. J. Immunol. 178, 271–279.

Webster, K.E., Walters, S., Kohler, R.E., Mrkvan, T., Boyman, O., Surh, C.D., Grey, S.T., Sprent, J., 2009. In vivo expansion of T reg cells with IL-2-mAb complexes: induction of resistance to EAE and long-term acceptance of islet allografts without immunosuppression. J. Exp. Med. 206, 751–760.

Wilson, M.S., Pesce, J.T., Ramalingam, T.R., Thompson, R.W., Cheever, A., Wynn, T.A., 2008. Suppression of murine allergic airway disease by IL-2:anti-IL-2 monoclonal antibody-induced regulatory T cells. J. Immunol. 181, 6942–6954.

Wohlfert, E.A., Grainger, J.R., Bouladoux, N., Konkel, J.E., Oldenhove, G., Ribeiro, C.H., Hall, J.A., Yagi, R., Naik, S., Bhairavabhotla, R., Paul, W.E., Bosselut, R., Wei, G., Zhao, K., Oukka, M., Zhu, J., Belkaid, Y., 2011. GATA3 controls $Foxp3^{(+)}$ regulatory T cell fate during inflammation in mice. J. Clin. Investig. 121, 4503–4515.

Wüst, S., van den Brandt, J., Tischner, D., Kleiman, A., Tuckermann, J.P., Gold, R., Lühder, F., Reichardt, H.M., 2008. Peripheral T cells are the therapeutic targets of glucocorticoids in experimental autoimmune encephalomyelitis. J. Immunol. 180 (12), 8434–8443.

Xie, Y., Wu, M., Song, R., Ma, J., Shi, Y., Qin, W., Jin, Y., 2009. A glucocorticoid amplifies IL-2-induced selective expansion of $CD4^{(+)}CD25^{(+)}FOXP3^{(+)}$ regulatory T cells in vivo and suppresses graft-versus-host disease after allogeneic lymphocyte transplantation. Acta Biochim. Biophys. Sin. 41, 781–791.

Yoshimoto, T., Yoshimoto, T., Yasuda, K., Mizuguchi, J., Nakanishi, K., 2007. IL-27 suppresses Th2 cell development and Th2 cytokines production from polarized Th2 cells: a novel therapeutic way for Th2-mediated allergic inflammation. J. Immunol. 179, 4415–4423.

Yu, A., Zhu, L., Altman, N.H., Malek, T.R., 2009. A low interleukin-2 receptor signaling threshold supports the development and homeostasis of T regulatory cells. Immunity 30, 204–217.

Zhao, J., Fett, C., Trandem, K., Fleming, E., Perlman, S., 2011. IFN-gamma- and IL-10-expressing virus epitope-specific $Foxp3^{(+)}$ T reg cells in the central nervous system during encephalomyelitis. J. Exp. Med. 208, 1571–1577.

Zhou, X., Bailey-Bucktrout, S.L., Jeker, L.T., Penaranda, C., Martinez-Llordella, M., Ashby, M., Nakayama, M., Rosenthal, W., Bluestone, J.A., 2009. Instability of the transcription factor Foxp3 leads to the generation of pathogenic memory T cells in vivo. Nat. Immunol. 10, 1000–1007.